# Wnt3a Reestablishes Osteogenic Capacity to Bone Grafts from Aged Animals

Philipp Leucht, MD*, Jie Jiang, PhD*, Du Cheng, BS*, Bo Liu, DDS, PhD*, Girija Dhamdhere, PhD, Mark Yang Fang, BS, Stefanie D. Monica, BS, Jonathan J. Urena, BS, Whitney Cole, BS, Lane R. Smith, PhD, Alesha B. Castillo, PhD, Michael T. Longaker, MD, MBA, and Jill A. Helms, DDS, PhD

*Investigation performed at the Department of Orthopaedic Surgery, and Division of Plastic and Reconstructive Surgery, Department of Surgery, Stanford School of Medicine, Stanford, California*

**Background:** Age-related fatty degeneration of the bone marrow contributes to delayed fracture-healing and osteoporosis-related fractures in the elderly. The mechanisms underlying this fatty change are unknown, but they may relate to the level of Wnt signaling within the aged marrow cavity.

**Methods:** Transgenic mice were used in conjunction with a syngeneic bone-graft model to follow the fates of cells involved in the engraftment. Immunohistochemistry along with quantitative assays were used to evaluate Wnt signaling and adipogenic and osteogenic gene expression in bone grafts from young and aged mice. Liposomal Wnt3a protein (L-Wnt3a) was tested for its ability to restore osteogenic potential to aged bone grafts in critical-size defect models created in mice and in rabbits. Radiography, microquantitative computed tomography (micro-CT) reconstruction, histology, and histomorphometric measurements were used to quantify bone-healing resulting from L-Wnt3a or a control substance (liposomal phosphate-buffered saline solution [L-PBS]).

**Results:** Expression profiling of cells in a bone graft demonstrated a shift away from an osteogenic gene profile and toward an adipogenic one with age. This age-related adipogenic shift was accompanied by a significant reduction ($p < 0.05$) in Wnt signaling and a loss in osteogenic potential. In both large and small animal models, osteogenic competence was restored to aged bone grafts by a brief incubation with the stem-cell factor Wnt3a. In addition, liposomal Wnt3a significantly reduced cell death in the bone graft, resulting in significantly more osseous regenerate in comparison with controls.

**Conclusions:** Liposomal Wnt3a enhances cell survival and reestablishes the osteogenic capacity of bone grafts from aged animals.

**Clinical Relevance:** We developed an effective, clinically applicable, regenerative medicine-based strategy for revitalizing bone grafts from aged patients.

In youth, long bones are filled with heme-rich marrow; with age, this is replaced by fatty marrow[1]. Age-related fatty degeneration of the bone marrow[2-4] is strongly associated with delayed skeletal healing and osteoporosis-related fractures in the elderly[5-8], which together constitute a growing biomedical burden[9,10]. Consequently, considerable research has been done in an attempt to understand the mechanism behind the conversion of bone marrow into predominantly fatty tissue.

This fatty degeneration of the bone marrow occurs in parallel with a loss in osteogenic potential[11-14], which is revealed when marrow is used clinically for bone-grafting purposes. A patient's own bone and marrow is considered the "gold standard,"[15] but these autografts are oftentimes inadequate when the patient is elderly[16].

There are multiple, distinct stem-cell and/or progenitor cell populations, including mesenchymal stem cells, that reside in the bone marrow[17-21]. Although mesenchymal stem cells can give rise to cartilage, bone, fat, and muscle cells when cultured in vitro, mesenchymal stem cells residing in the marrow cavity itself only differentiate into an osteogenic or an adipogenic

*Philipp Leucht, MD, Jie Jiang, PhD, Du Cheng, BS, and Bo Liu, DDS, PhD contributed equally to the preparation of this article.

**Disclosure:** One or more of the authors received payments or services, either directly or indirectly (i.e., via his or her institution), from a third party in support of an aspect of this work. In addition, one or more of the authors, or his or her institution, has had a financial relationship, in the thirty-six months prior to submission of this work, with an entity in the biomedical arena that could be perceived to influence or have the potential to influence what is written in this work. No author has had any other relationships, or has engaged in any other activities, that could be perceived to influence or have the potential to influence what is written in this work. The complete **Disclosures of Potential Conflicts of Interest** submitted by authors are always provided with the online version of the article.

lineage[22], and growing evidence indicates that this adipogenic-osteogenic fate decision is regulated by beta-catenin-dependent Wnt signaling[23]. For example, enhancing Wnt signaling by activating mutations in the Wnt low-density lipoprotein receptor-related protein-5 (LRP5) receptor[24] causes a high bone-mass phenotype in humans[25,26]. In vitro, this same activating mutation represses adipocyte differentiation of human mesenchymal stem cells[27]. On the other hand, reduced Wnt signaling (for example, as occurs with the osteolytic disease multiple myeloma[28]) is associated with aggressive bone loss[29] and a concomitant increase in marrow adiopogenesis at the expense of hematopoiesis[30]. Together, these observations support a hypothesis that Wnt signaling has a positive role in stimulating osteogenesis[31] and inhibiting adipogenesis[32].

We employed an in vivo, syngeneic transplantation assay[33] to gain mechanistic insights into the age-related fatty degeneration of the marrow and its concomitant loss of osteogenic potential. We employed two animal models that are based on a standard bone-grafting procedure, a technique that is performed more than 500,000 times annually in the U.S. alone[34]. We identified a correlation between diminished Wnt signaling and fatty degeneration of the marrow, and we then used those findings to formulate a treatment approach to re-establish Wnt responsiveness and bone-forming capacity to bone grafts from aged animals.

## Materials and Methods

### Animals

All procedures were approved by the Stanford Committee on Animal Research. Axin2$^{LacZ/+}$ mice have been described[35]. Beta-actin-enhanced green fluorescent protein (ACTB-eGFP) transgenic mice (The Jackson Laboratory, Sacramento, California) were chosen because of robust expression levels of GFP in bone, marrow, and other relevant cell populations[36]. ACTB-eGFP transgenic mice were crossed with *Axin2*$^{LacZ/+}$ mice to obtain *Axin2*$^{LacZ/+}$, Axin2$^{LacZ/+}$/ACTB-eGFP, ACTB-eGFP and wild-type (WT) mice; twelve to sixteen weeks old mice were considered young; mice greater than forty weeks of age were considered aged. Aged (eight months) New Zealand white rabbits were used. One rabbit served as the bone graft donor, and nine rabbits served as experimental animals.

### Bone-Grafting in Mice

Host mice (male only) were anesthetized by intraperitoneal injection of ketamine (80 mg/kg) and xylazine (16 mg/kg). A 3-mm incision was made to expose the parietal bone; a circumferential, full-thickness defect with a 2-mm diameter was created with use of a micro dissecting trephine; the dura mater was not disturbed.

Bone graft was harvested from the femora and tibiae, pooled, and divided into aliquots. Each 20-μL aliquot was incubated in 10 μL of Dulbecco modified Eagle Medium (DMEM) with 10% fetal bovine serum (FBS) containing liposomal phosphate-buffered saline solution (L-PBS) or liposomal Wnt3a protein (L-Wnt3a) (effective concentration = 0.15 μg/mL) at 37°C while the calvarial defect was prepared. Bone grafts were transplanted to the calvarial defect, and the skin was closed.

### Bone-Grafting in Rabbits

Host rabbits were anesthetized with a subcutaneous injection of glycopyrrolate (0.02 mg/kg) and buprenorphine (0.05 mg/kg), an intramuscular injection of ketamine (35 mg/kg) and xylazine (5 mg/kg), and an intravenous injection of cefazolin (20 mg/kg), and maintained under 1% to 3% isoflurane. A 2.5-cm incision was made, the ulnar border was visualized, and a 1.5-cm segmental defect was created with an oscillating saw (Stryker System 5, Kalamazoo, Michigan). The segment was removed along with its periosteal tissues. Bone graft was harvested from the pelvis and femur, pooled, and divided into aliquots. Each approximately 400-mg aliquot was combined with L-PBS (500 μL) or L-Wnt3a (effective concentration = 0.5 μg/mL) and kept on ice on the back table while the ulnar defect was created in host rabbits. Bone grafts were transplanted to the ulnar defect, and the muscle and skin were closed. The procedure was performed bilaterally (i.e., both sides either received L-PBS or L-Wnt3a). This approach eliminated the possibility, however remote, that the bone graft would have an unanticipated systemic effect.

### In Vitro Wnt Stimulation of Rabbit Bone Marrow

Bone marrow from aged rabbits was incubated with L-PBS or L-Wnt3a (effective concentration = 0.15 μg/mL) at 37°C for twelve hours. Total DNA was assayed with use of PicoGreen dsDNA kit (Life Technologies, Carlsbad, California) to ensure that grafts had equivalent cell volumes. Caspase activity was assayed with use of a standard kit (Roche Diagnostics, Indianapolis, Indiana).

### Tissue Preparation

Immediately after euthanasia (time points specified in each experiment), the entire skeletal element, including muscle, connective tissue, and/or dura was harvested, removed of its epidermis, and fixed in 4% paraformaldehyde at 4°C for twelve hours. Samples were decalcified in 19% EDTA (ethylenediaminetetraacetic acid) before embedding in paraffin, or in optimal cutting temperature (OCT) compound. Sections were 10-μm thick.

### Histology, Immunohistochemistry, and Histomorphometric Analyses

Immunohistochemistry was performed as previously described[31]. Antibodies used included rabbit polyclonal anti-green fluorescent protein (anti-GFP) (Cell Signaling Technology, Danvers, Massachusetts), rabbit polyclonal anti-DLK1 (EMD Millipore, Billerica, Massachusetts), anti-peroxisome proliferator activated receptor-γ (anti-PPAR-γ) (Millipore), and anti-Ki67 (ThermoFisher Scientific, Waltham, Massachusetts). The bromodeoxyuridine (BrdU) (Invitrogen, Camarillo, California) and terminal deoxynucleotidyl transferase dUTP nick end labeling (TUNEL) (Roche Diagnostics) assays were performed following the manufacturers' instructions.

Movat pentachrome, aniline blue, Xgal, and alkaline phosphatase (ALP) stainings were performed as previously described[31]. Tissue sections were photographed with use of a Leica DM5000B digital imaging system (Leica Microsystems, Wetzlar, Germany). A minimum of five tissue sections per sample was used for histomorphometric analyses[37].

### Microquantitative Computed Tomography (Micro-CT) Analyses

Mice were anesthetized with 2% isoflurane and scanned with use of a multimodal positron emission tomography-computed tomography data-acquisition system (Inveon PET-CT; Siemens, Erlangen, Germany) at 40-μm resolution. Data were analyzed with MicroView software (GE Healthcare, Chicago, Illinois). The three-dimensional region-of-interest tool was used to assign the structure and bone volume for each sample.

Assessment of the regenerate bone volume fraction (the percentage calculated by dividing the total bone volume by the regenerate bone volume [BV/TV, %]) was performed with use of high-resolution micro-CT (vivaCT 40; Scanco Medical, Brüttisellen, Switzerland) and with 70 kVp, 55 μA, 200-ms integration time, and a 10.5-μm isotropic voxel size. The region of interest was 2 cm in length and began 250 μm proximal to the edge of the defect and extended 250 μm distally beyond the opposing edge of the defect (1.5 cm total diameter). Bone was segmented from soft tissue with use of a threshold of 275 mg/cm$^3$ hydroxyapatite. Scanning and analyses adhered to published guidelines[38].

### Quantitative Reverse Transcription-Polymerase Chain Reaction (qRT-PCR)

Tissue samples were homogenized in TRIzol solution (Life Technologies). RNA was isolated (RNeasy; Qiagen, Germantown, Maryland) and reverse transcription was performed (SuperScript III Platinum Two-Step qRT-PCR Kit, Life Technologies) as described previously[31]. Primer sequences are listed in Figure E-1 in Appendix.

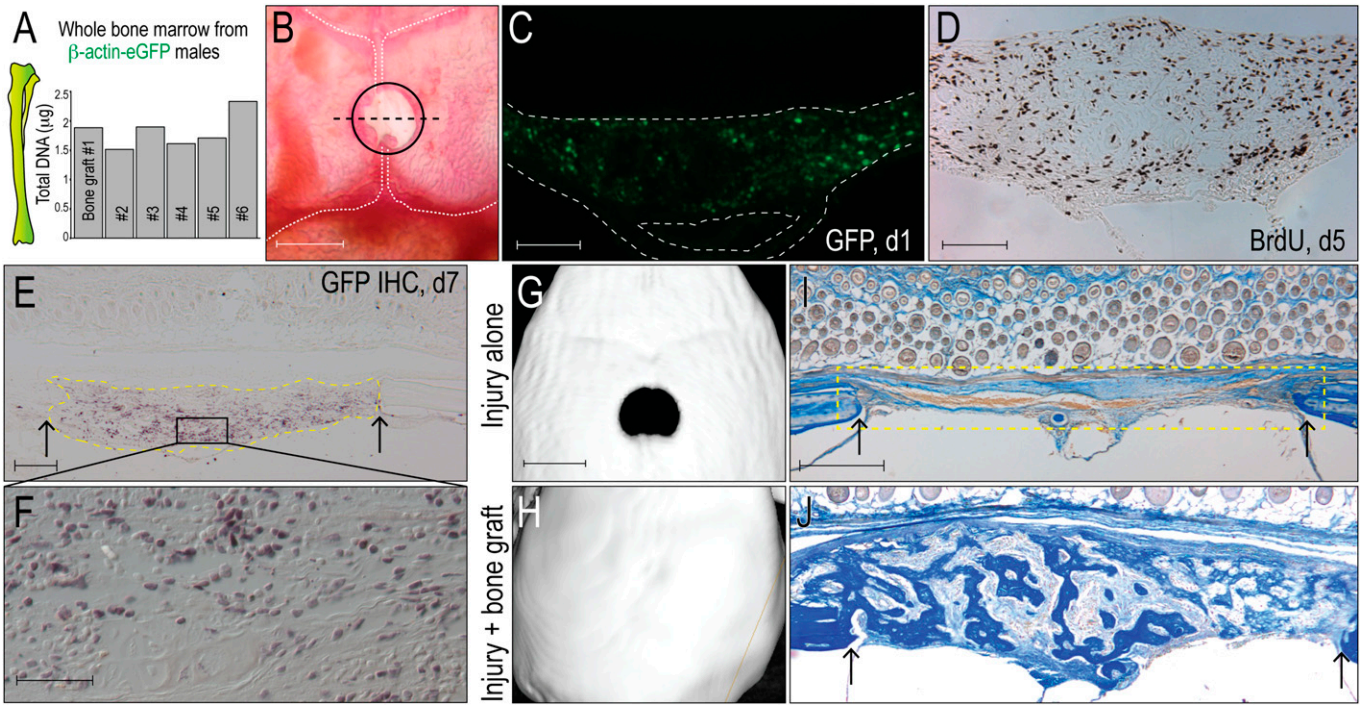


Fig. 1

Bone grafts have osteogenic potential. **Fig. 1-A** Quantification of total DNA in representative aliquots of whole bone marrow harvested from transgenic beta-actin-enhanced green fluorescent protein (β-actin-eGFP) male mice; each aliquot constitutes a bone graft. **Fig. 1-B** Bone grafts are transplanted into 2-mm-diameter critical-size calvarial defects (demarcated with a circle), which are created in the sagittal suture that separates the parietal bones (outlined with vertical white dashed lines). The dashed black line indicates the plane of tissue section. **Fig. 1-C** Representative tissue section from the injury site on post-transplant day 1; GFP immunostaining identifies grafted cells from the eGFP donor (n = 5); the inferior space represents the sagittal sinus. **Fig. 1-D** Representative tissue section on post-transplant day 5; immunostaining for bromodeoxyuridine (BrdU) identifies cells in S phase. **Fig. 1-E** On post-transplant day 7, GFP immunostaining identifies the bone graft (dotted yellow line); a higher magnification image of the boxed area in Fig. 1-E (**Fig. 1-F**) illustrates that the majority of the cells in the injury site are derived from GFP-positive graft. **Fig. 1-G** On post-transplant day 14, micro-CT reconstruction confirms that a 2-mm calvarial injury constitutes a critical-size nonhealing defect (n = 6)[40]. **Fig. 1-H** The same size calvarial injury, treated with a bone graft, heals (n = 6). **Figs. 1-I and 1-J** On post-transplant day 7, aniline blue staining was used to identify new osteoid matrix; no osteoid matrix formed in the untreated injury site (yellow dotted line). **Fig. 1-J** shows visible osteoid matrix on post-transplant day 7 in a representative sample that had been treated with a bone graft. Abbreviations: IHC = immunohistochemistry. Arrows mark the edges of intact bone. Scale bars: 2 mm (Fig. 1-B); 200 µm (Figs. 1-C and 1-D); 100 µm (Fig. 1-E); 40 µm (Fig. 1-F); 2 mm (Fig. 1-G); and 200 µm (Fig. 1-I).

### *Statistical Analyses*

Results are presented as the mean plus the standard deviation, with "n" signifying the number of samples analyzed. Significant differences between data sets were determined with use of two-tailed Student t tests and nonparametric Wilcoxon tests. Significance was attained at $p < 0.05$, and all statistical analyses were performed with GraphPad Prism software (GraphPad Software, San Diego, California).

### *Source of Funding*

Work was funded by the California Institute for Regenerative Medicine (CIRM) TR1-0219. P. Leucht received funding from the Orthopaedic Research and Education Foundation (OREF) in the form of a Career Development Award in Total Joint and Trauma Surgery (OREF grant #10-006). J. Jiang was funded by a National Institutes of Health Ruth L. Kirschstein National Research Service Award (NRSA) 5F32AR57648-2. D. Cheng and W. Cole are California Institute for Regenerative Medicine (CIRM) Bridges to Stem Cell Research Certificate Program Scholars (TB1-01190 and TB1-01175). Neither the authors' employment at Stanford University nor any grants or patents pending played any role in the reporting of the study.

## Results

### *Bone-Marrow Grafts Have Osteogenic Potential*

To follow the fate of the bone-graft material, we harvested whole bone marrow from ACTB-eGFP transgenic mice[36,39], subdivided it into equivalent-size aliquots (Fig. 1-A), then transplanted it into a nonhealing, critical-size skeletal defect[40] that was created in the calvarium of syngeneic host mice (Fig. 1-B). The viable grafted cells and their progeny were identifiable within the injury site by their GFP label (Fig. 1-C). When the donor and host were not genetically identical, most of the grafted cells died (not shown); for that reason, only syngeneic, immunologically compatible donor-host combinations were used.

On post-graft day 1, GFP-positive cells, along with stromal tissue from the GFP-positive donor, occupied the injury site (Fig. 1-C). On day 5, BrdU staining confirmed the robust proliferation of cells in the defect site (Fig. 1-D). On day 7, GFP immunostaining confirmed that grafted cells, or their

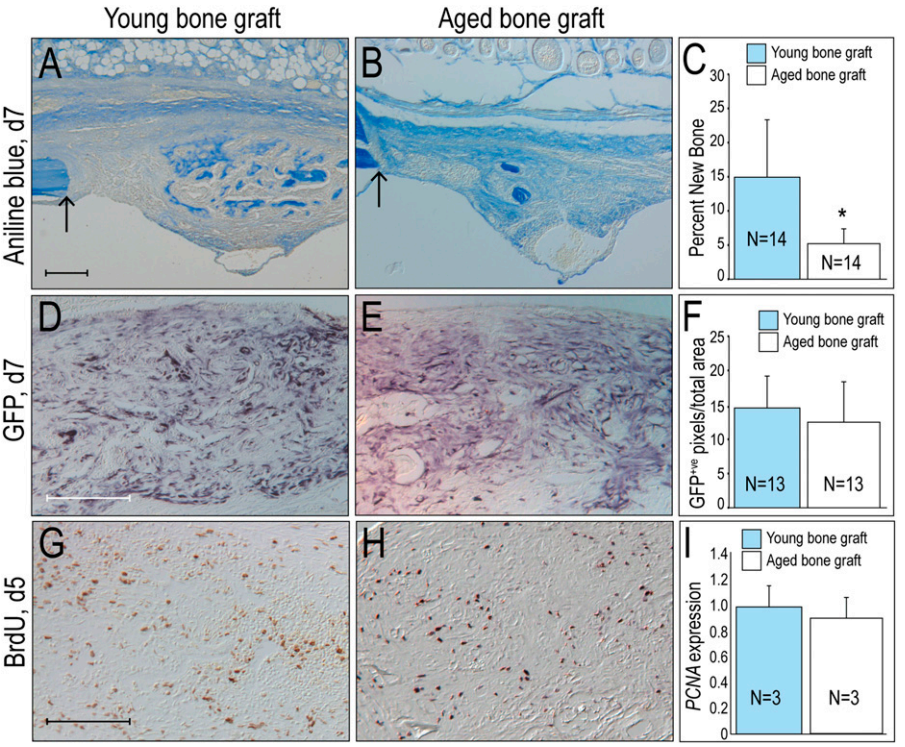


Fig. 2

Osteogenic potential is reduced in bone grafts from aged animals. On post-transplant day 7 (d7), aniline blue staining indicates osteoid matrix generated by bone grafts from young (**Fig. 2-A**) versus aged donors (**Fig. 2-B**). **Fig. 2-C** Histomorphometric analyses of the amount of new bone formed from young and aged bone grafts. **Fig. 2-D** On post-transplant day 7 (d7), green fluorescent protein (GFP) immunostaining identifies cells derived from the bone graft when the donor is young as compared with aged (**Fig. 2-E**). **Fig. 2-F** The number of GFP-positive ($GFP^{+ve}$) cells in the injury site when the graft is harvested from young (blue bars, n = 13) compared with aged (white bars, n = 13) donors. On post-transplant day 5 (d5), bromodeoxyuridine (BrdU) staining identifies proliferating cells in bone grafts from young (**Fig. 2-G**) and aged (**Fig. 2-H**) donors. **Fig. 2-I** Quantitative reverse transcription-polymerase chain reaction (qRT-PCR) for proliferating cell nuclear antigen (PCNA) in bone grafts from young and aged animals are equivalent. Single asterisk denotes $p < 0.05$. Arrow marks the edge of intact bone. Scale bars: 200 μm (Figs. 2-A, [scale bar in Fig. 2-A also applies to Fig. 2-B], 2-D [scale bar in Fig. 2-D also applies to Fig. 2-E], and 2-G [scale bar in Fig. 2-G also applies to Fig. 2-H]).

progeny, remained at the defect site (Figs. 1-E and 1-F). The grafted cells and/or their progeny eventually differentiate into osteoblasts and heal the defect (Figs. 1-H and 1-J); in the absence of a bone graft, the defect will not heal (Figs. 1-G and 1-I)[40,41].

### *Aged Bone Grafts Exhibit Fatty Degeneration*

With aging, human bone marrow undergoes fatty degeneration and a loss in osteogenic potential[42]. A comparable age-related change is observed in mice, in which the gross appearance of murine bone marrow changes from a heme-rich, fat-free tissue in young animals to a fatty marrow in aged animals (Figs. E-2A, E-2B, and E-2C in Appendix). Quantitative RT-PCR analyses of the heterogeneous cell population that constitutes a bone graft showed that relative to samples from young animals, samples from aged animals showed significantly higher expression of the adipogenic genes fatty acid-binding protein 4 (Fabp4) ($p < 0.01$) and peroxisome proliferator-activated receptor gamma (PPAR-γ) ($p < 0.01$; Fig. E-2D in Appendix). Simultaneous with this adipogenic shift, bone grafts from aged mice also showed significantly reduced expression levels of the osteogenic genes ALP ($p < 0.05$), osteocalcin ($p < 0.01$), and osterix ($p < 0.05$; Fig. E-2E in Appendix). Thus, fatty degeneration of the bone marrow observed in humans is recapitulated in mice at both a gross morphologic level and at a quantifiable, molecular level.

### *Fatty Degeneration Is Associated with Reduced Osteogenic Potential in a Bone Graft*

Compared with the osteogenic capacity of grafts from young animals, grafts from aged animals generated significantly less new bone (Figs. 2-A and 2-B; quantified in 2-C; $p < 0.05$). This age-related reduction in osteogenic potential was not directly attributable to differences in engraftment efficiency. Using GFP immunostaining to identify the grafted cells, the distribution and number of GFP-positive cells was nearly equivalent between bone grafts from young and aged mice (Figs. 2-D and 2-E; quantified in 2-F). Nor was the age-related alteration in osteogenic potential attributable to differences in the expansion of the graft: Using both BrdU incorporation (Figs. 2-G and 2-H) and qRT-PCR for proliferating cell nuclear antigen

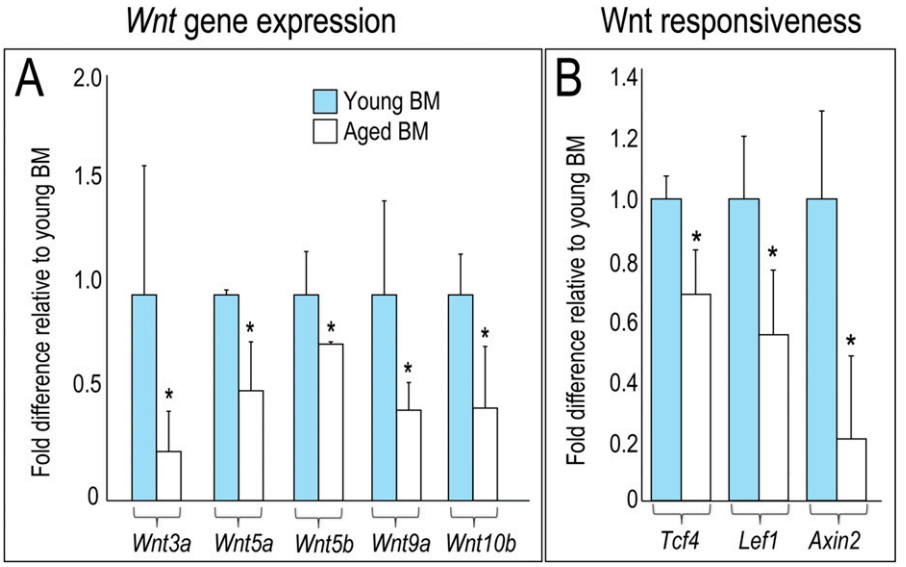


Fig. 3

Wnt signaling is reduced in aged bone grafts. **Fig. 3-A** Quantitative RT-PCR to evaluate relative expression levels of Wnt ligands and Wnt target (**Fig. 3-B**) genes in bone marrow (BM) harvested from young (blue bars; n = 3) and aged (white bars; n = 3) donors. Gene expression levels normalized to glyceraldehyde 3-phosphate dehydrogenase (GAPDH). Asterisk denotes $p < 0.05$.

(PCNA) (Fig. 2-I) we found nearly equivalent levels of cell proliferation in bone grafts from young and aged animals.

We gained insights into the basis for fatty degeneration and loss in osteogenic potential of aged bone grafts when we assessed the expression level of nineteen mammalian *Wnt* genes in marrow cells. A subset of *Wnt* genes were weakly expressed in bone marrow from aged animals compared with young animals ($p < 0.05$; Fig. 3-A). This reduction in *Wnt* gene expression was paralleled by a reduction in Wnt responsiveness, as measured by significantly decreased expression of the Wnt direct target genes *Tcf4, Lef1,* and *Axin2* ($p < 0.05$; Fig. 3-B). These results demonstrate that Wnt signaling is reduced in aged bone marrow.

### *L-Wnt3a Restores Osteogenic Capacity to Bone Grafts from Aged Mice*

The first Wnt protein to be purified was Wnt3a[43]. Wnt3a acts via the "canonical" or beta-catenin dependent pathway[44] and is a well-known osteogenic stimulus[45]. Given the reduced Wnt signaling in aged bone marrow, we wondered if the addition of exogenous Wnt protein would be sufficient to reestablish the osteogenic potential of bone grafts derived from aged animals.

All vertebrate Wnt proteins are hydrophobic[46]; without a carrier, the hydrophobic Wnt3a rapidly denatures and becomes inactive[31,47,48]. We solved this in vivo delivery problem by packaging the hydrophobic Wnt3a in lipid particles. This formulation of the human Wnt3a protein, liposomal Wnt3a (L-Wnt3a), is stable in vivo[49] and promotes robust bone regeneration in a modified fracture model[31]. Although exogenously applied Wnt3a has great potential as a therapeutic protein, safety remains a primary concern. The delivery of high concentrations of potent growth factors to a skeletal injury site carries with it potential oncological risk to the patient[50]. To circumvent issues associated with prolonged or uncontrolled exposure to a growth factor, we delivered L-Wnt3a ex vivo. This was accomplished by incubating the aged bone graft with L-Wnt3a (n = 30) immediately after harvest, while the recipient site was prepared. Control bone grafts were exposed to L-PBS (n = 30) for the same duration.

Compared with aged grafts treated with L-PBS (Fig. 4-A), aged grafts treated with L-Wnt3a showed a dramatic enhancement in new bone formation (Fig. 4-B). Within seven days, defect sites that received L-Wnt3a-treated grafts had twofold more new bone than sites that received L-PBS treated grafts (Fig. 4-C). By day 12, L-Wnt3a-treated grafts had 1.5-fold more new bone compared with L-PBS treated grafts (Fig. 4-D and 4-E; quantified in 4-C).

### *Bone-Marrow-Derived Stem Cells Are Wnt Responsive*

To gain insights into which cell population(s) in the bone graft responded to the Wnt stimulus, we assayed different fractions of the marrow for Wnt responsiveness. In whole bone marrow, Wnt responsiveness was below detectable levels. We separated whole bone marrow[51] into a nonadherent population[52]; once again Wnt responsiveness was below the limit of detection (Fig. 4-F). In the adherent population, however, which contains connective tissue progenitor cells[53,54], Wnt responsiveness was detected (Fig. 4-F). We then used established protocols[51] to further enrich for bone-marrow stem and/or stromal cells from the attached population. Using immunostaining for CD45(–), CD73(+), CD105(+), and Stro1(+), we confirmed that this population was enriched for marrow-derived stem cells[55,56] (Fig. 4-G). Relative to PBS-treated CD45(–), CD73(+), CD105(+), and Stro1(+) cells, the Wnt3a-treated population showed a tenfold increase in Wnt responsiveness (Fig. 4-H).

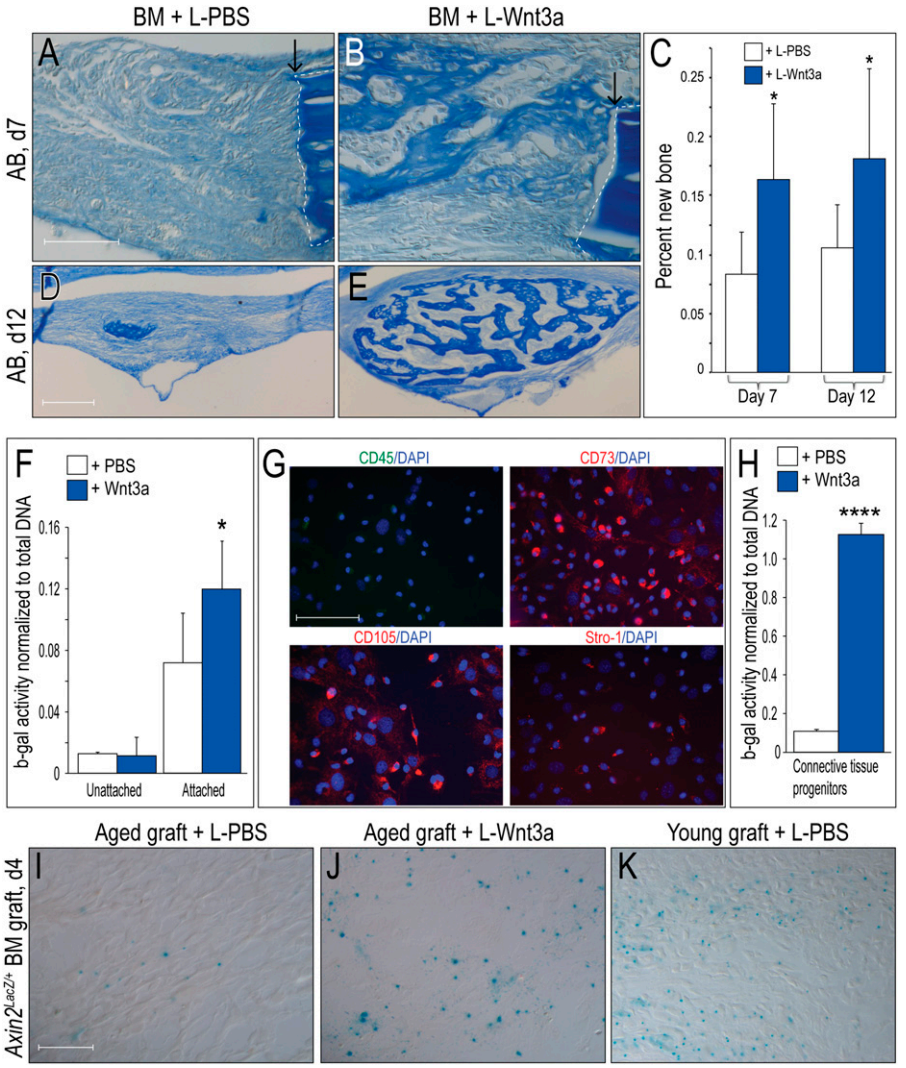


Fig. 4

Liposomal Wnt3a restores osteogenic capacity to aged bone grafts. **Fig. 4-A** Aniline blue staining of L-PBS treated aged bone grafts (n = 5). **Fig. 4-B** New aniline-blue positive osteoid matrix in L-Wnt3a treated bone grafts (n = 8). **Fig. 4-C** Histomorphometric quantification of new bone matrix on post-transplant days seven and twelve. **Fig. 4-D** Aniline blue staining on post-transplant day twelve (d12) in L-PBS and L-Wnt3a (**Fig. 4-E**) treated bone grafts. **Fig. 4-F** Beta galactosidase (b-gal) activity normalized to total DNA as measured in cell populations (unattached, floating cells and attached cells) from a bone marrow harvest. White bars (n = 4) represent Wnt responsiveness following L-PBS treatment; blue bars (n = 4) represent Wnt responsiveness following L-Wnt3a treatment (effective concentration 0.15 μg/mL Wnt3a). **Fig. 4-G** Immunostaining for the stem cell markers CD45, CD73, CD105, and Stro1 in attached cells derived from the bone marrow. **Fig. 4-H** Beta galactosidase activity normalized to total DNA in the attached cell population following L-PBS treatment (white bars, n = 4) or following L-Wnt3a treatment (n = 4; effective concentration 0.15 μg/mL Wnt3a). **Fig. 4-I** Xgal staining on a representative tissue section identifies Wnt responsive cells in a bone graft from an aged $Axin2^{LacZ/+}$ mouse treated with L-PBS, compared with treatment with L-Wnt3a (**Fig. 4-J**). **Fig. 4-K** Xgal staining on a representative tissue section identifies Wnt responsive cells in an L-PBS-treated bone graft from a young $Axin2^{LacZ/+}$ mouse. Single asterisk denotes $p < 0.05$; quadruple asterisk denotes $p \leq 0.0001$. Abbreviations: L-PBS = liposomal PBS; L-Wnt3a = liposomal Wnt3a; BM = bone marrow; and DAPI = 4',6-diamidino-2-phenylindole, dihydrochloride. Arrows mark the edges of intact bone. Scale bars: 100 μm (Figs. 4-A [scale bar in Fig. 4-A also applies to Fig. 4-B]); 200 μm (Figs. 4-D [scale bar in Fig. 4-D also applies to Fig. 4-E]); 100 μm (Fig. 4-G); and 40 μm (Figs. 4-I, [scale bar in Fig. 4-I also applies to Figs. 4-J and 4-K]).

We also monitored Wnt responsiveness in bone grafts using Xgal staining of marrow from $Axin2^{LacZ/+}$ mice[31,35,57]. Very few $Xgal^{+ve}$ cells were found in aged bone grafts (Fig. 4-I) but $Xgal^{+ve}$ cells were plentiful in young bone grafts (Fig. 4-K). Aged bone grafts were capable of responding to an L-Wnt3a stimulus, as shown by the increase in $Xgal^{+ve}$ cells following exposure (Fig. 4-J). Because the prevalence of stem cells in the murine marrow cavity is quite low[58], it is likely that the Wnt responsive population included more cells than the CD45(–), CD73(+), CD105(+), and Stro1(+) population.

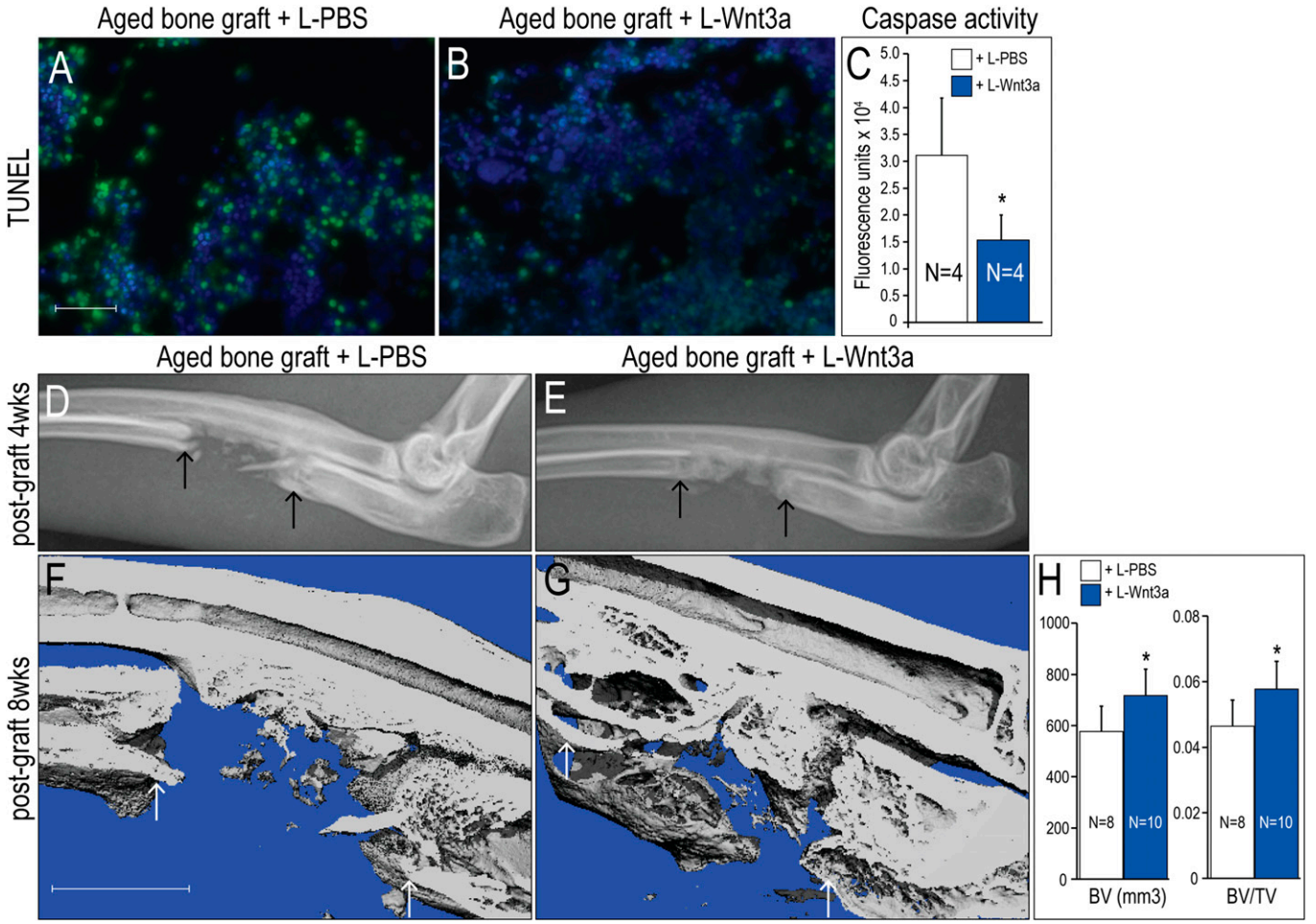


Fig. 5

L-Wnt3a treatment restores osteogenic potential to bone grafts from aged animals. Bone marrow from aged donor rabbits, assayed for DNA fragmentation associated with cell apoptosis. **Fig. 5-A** Terminal deoxynucleotidyl transferase dUTP nick end labeling (TUNEL) staining (n = 4) demonstrates the extent of apoptosis in aged bone marrow treated with L-PBS (10 μL), compared with L-Wnt3a (**Fig. 5-B**) treatment (effective concentration = 0.15 μg/mL Wnt3a). **Fig. 5-C** A measurement of caspase activity in aged bone graft samples treated with L-PBS (white bars) or L-Wnt3a (blue bars). Figs. **5-D through 5-G** Bone marrow was harvested from aged rabbits, incubated with L-PBS or L-Wnt3a for up to 1h, then transplanted into a critical-size defect created in the ulna. **Fig. 5-D** Radiographic assessment at four weeks following bone-grafting. Compare L-PBS treatment with L-Wnt3a (**Fig. 5-E**) treatment. **Fig. 5-F** Micro-CT iso-surface reconstruction at eight weeks following bone-grafting. Compare L-PBS treatment with L-Wnt3a (**Fig. 5-G**) treatment. **Fig. 5-H** Bone volume (BV) and bone volume/total volume (BV/TV) are calculated using the bone analysis tool in GE MicroView software. A single asterisk denotes $p < 0.05$. Abbreviations: L-PBS = liposomal PBS and L-Wnt3a = liposomal Wnt3a. Arrows mark the edge of intact bone. Scale bars: 40 μm (Figs. 5-A and 5-B); and 5 mm (Figs. 5-F and 5-G).

### *L-Wnt3a Prevents Apoptosis in Bone Grafts*

The robust bone-inducing capacity of L-Wnt3a prompted us to extend our studies into a large animal, long-bone model[59]. As in humans, aged rabbits experience fatty degeneration of their marrow[60,61]. We utilized a critical-size ulnar defect model[62] and transplanted aged bone grafts that had been incubated with L-PBS or L-Wnt3a into the defect. We first noted that when bone graft is harvested there is extensive programmed cell death throughout the aggregate (Fig. 5-A; see Fig. E-2 in Appendix). The addition of L-Wnt3a significantly reduced this graft apoptosis ($p < 0.05$) (Fig. 5-B; see Fig. E-2 in Appendix). We verified this pro-survival effect of L-Wnt3a, using caspase activity as a measure of cell apoptosis[63,64]. L-Wnt3a significantly reduced caspase activity in cells of the bone graft ($p < 0.05$; Fig. 5-C).

### *L-Wnt3a Potentiates the Osteogenic Capacity of Aged Bone Grafts*

L-Wnt3a and L-PBS-treated rabbit bone grafts were introduced into the critical size defect and regeneration was assessed at multiple time points. Radiographic assessment at four weeks revealed the presence of a bridging callus in sites that had received L-Wnt3a-treated graft (Fig. 5-E); in comparison, sites that received L-PBS-treated bone graft showed minimal callus formation (Figs. 5-D).

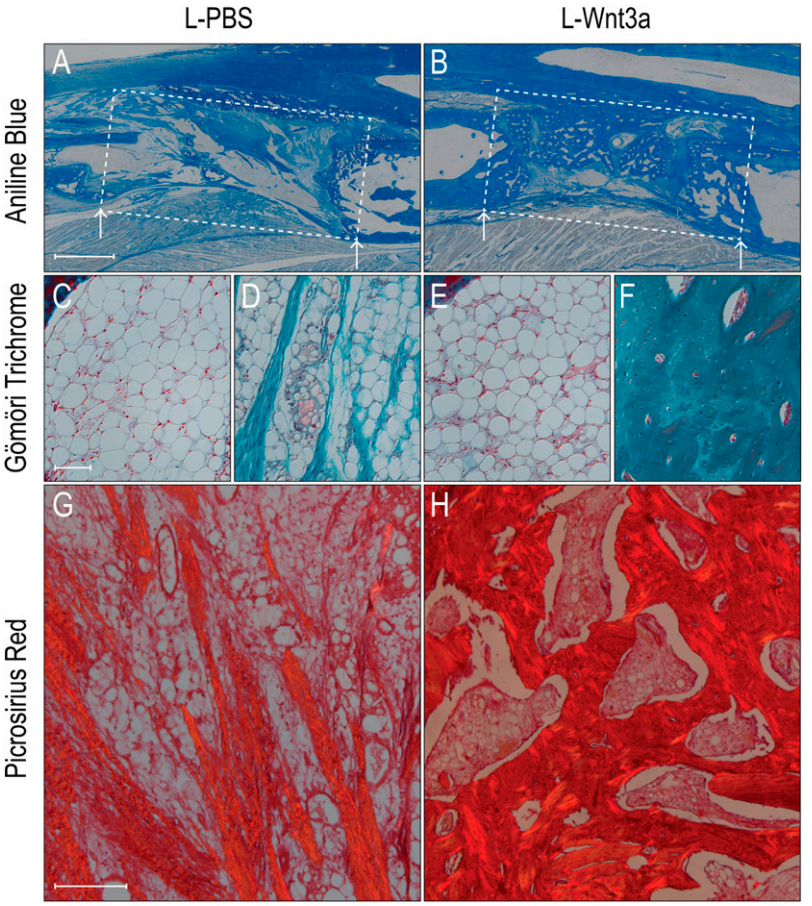


Fig. 6

Histological appearance of regenerated bone derived from L-Wnt3a treated aged bone grafts. Aniline blue staining of injury site (boxed area) treated with aged bone marrow incubated in L-PBS (**Fig. 6-A)** or L-Wnt3a (**Fig. 6-B**). **Fig. 6-C** Gömöri trichrome staining of aged host's fatty bone marrow cavity, and the adjacent injury (**Fig. 6-D**) area that received an L-PBS treated aged bone graft; fibrous tissue is stained turquoise blue. **Fig. 6-E** Gömöri trichrome staining of aged host's fatty bone-marrow cavity, and the adjacent injury (**Fig. 6-F**) area that received an L-Wnt3a treated aged bone graft; mature osteoid matrix stains dark turquoise and osteocyte nuclei stain red. **Fig. 6-G** Under polarized light, picrosirius red staining identifies fibrous tissue that has formed from aged bone graft treated with L-PBS. Compare with the osteoid matrix (**Fig. 6-H**) that has formed from aged bone graft treated with L-Wnt3a. Abbreviations: L-PBS = liposomal PBS, and L-Wnt3a = liposomal Wnt3a. Arrows mark the edge of intact bone. Scale bars: 500 μm (Figs. 6-A and 6-B); 100 μm (Figs. 6-C through 6-F); and 200 μm (Figs. 6-G and 6-H).

At eight weeks, micro-CT analyses demonstrated a persistent gap in sites that were treated with L-PBS bone grafts (Fig. 5-F) whereas sites treated with L-Wnt3a bone graft exhibited robust bone formation (Fig. 5-G). Histomorphometric analyses confirmed a significant difference between the two groups, both in bone volume and in bone volume divided by total volume (Fig. 5-H).

We assessed the quality of the bone regenerate. Compared with controls (Fig. 6-A), L-Wnt3a-treated injury sites were filled with new bone (Fig. 6-B). The bone marrow of the host rabbits had undergone fatty degeneration (Fig. 6-C), and a similar appearance was noted in the L-PBS-treated regenerate (Fig. 6-D). In the L-Wnt3a treated samples (Fig. 6-E), the host bone marrow showed a similar level of fatty degeneration as seen in the control animals, but the regenerate from L-Wnt3a bone graft was woven bone (Fig. 6-F) and was distinguishable from the preexisting lamellar bone by both its location in the segmental defect site and its woven appearance (see Fig. E-3 in Appendix). Under polarized light, picrosirius red staining distinguished the mature, osteoid tissue found in the L-Wnt3a-treated bone grafts (Fig. 6-H) from the fibrous tissue of the L-PBS treated bone grafts (Fig. 6-G).

## Discussion

### *Stem-Cell and/or Progenitor Cell Populations in Bone Grafts*

The mammalian bone-marrow cavity is a functional niche that supports multiple stem-cell and/or progenitor cell populations[19,65]. Marrow-derived bone grafts, which are heterogeneous by nature, contain multiple populations, including some stem cells and/or progenitor cells. The contribution of these stem cells and/or progenitor cells to an osseous regenerate, however, remains unknown. Multiple marrow-derived

stem-cell populations are Wnt-responsive[66-70] and, using established protocols[51,56], we confirmed that at least the CD45(–), CD73(+), CD105(+), and Stro1(+) stem-cell and/or stromal-cell population in the bone marrow is Wnt-responsive (Fig. 4). Theoretically, this stem cell population could have contributed to the osseous regenerate but this remains to be demonstrated.

### *Wnt Signaling and Age-Related Fatty Degeneration of the Marrow*

In vitro, the abrogation of Wnt signaling causes mesenchymal stem cells to differentiate into adipocytes[71-73] whereas potentiation of Wnt signaling causes mesenchymal stem cells to differentiate into osteoblasts[74,75]. This may have direct clinical relevance: With age, human bone marrow undergoes fatty degeneration and loses its osteogenic potential (see Fig. E-2 in Appendix)[76]. Our data suggest that this loss in osteogenic potential of aged bone grafts rests, in part, on a reduced level of Wnt signaling: Compared with bone grafts from young mice, aged bone grafts show a dramatic reduction in *Wnt* gene expression and Wnt responsiveness (Fig. 3). Adding L-Wnt3a to aged bone marrow reestablishes its bone-forming capacity (Figs. 4, 5, and 6).

Conditions associated with decreased mobility, such as extended bed rest[77] and osteoporosis[60], are also associated with fatty degeneration of the marrow. Some data suggest that fatty degeneration is reversible, at least experimentally[78]. Clearly, understanding the basis for this degeneration—and the extent to which age-related changes in the skeleton can be reduced—will be of considerable importance in devising new treatment for bone injuries in elderly patients.

### *Growth-Factor-Augmented Bone Regeneration: Safety First*

Safety concerns have recently arisen surrounding the use of growth factors to augment skeletal healing[79-83]. Growth factor stimuli are largely thought to induce the proliferation of cells residing in the injury site; because uncontrolled proliferation is a characteristic of oncogenic transformation[84,85], this proliferative burst must be controlled both spatially and temporally.

For this reason, we designed an approach that would limit whole-body exposure to L-Wnt3a. The targeted cells are those in the bone graft itself, which is incubated with L-Wnt3a ex vivo. The activated cells—rather than the growth factor itself—are then reintroduced into a defect site. This ex vivo approach restricts the L-Wnt3a stimulus spatially (to the graft itself, and not to host tissues) and temporally (exposure to the Wnt stimulus only occurs during the incubation period). This ex vivo approach is tailored to clinical use and does not require a second procedure. Thus, packaging Wnt protein into lipoparticles constitutes a viable strategy for the treatment of skeletal injuries, especially those in individuals with diminished healing potential.

## Appendix

eA Figures showing evidence of the effect of L-Wnt3a on graft apoptosis are available with the online version of this article as a data supplement at jbjs.org. ■

Philipp Leucht, MD
Lane R. Smith, PhD
Department of Orthopaedic Surgery (P.L., L.R.S.),
Stanford School of Medicine, Stanford, CA 94305

Jie Jiang, PhD
Department of Bioengineering (J.J.),
University of California Los Angeles,
Los Angeles, CA 90095

Du Cheng, BS
Bo Liu, DDS, PhD
Girija Dhamdhere, PhD
Mark Yang Fang, BS
Michael T. Longaker, MD, MBA
Jill A. Helms, DDS, PhD
Division of Plastic and Reconstructive Surgery
(D.C., B.L., G.D., M.Y.F., M.T.L., J.A.H.),
Department of Surgery Stanford
School of Medicine, Stanford, CA 94305.
E-mail address for J.A. Helms: jhelms@stanford.edu

Stefanie D. Monica, BS
Department of Molecular and Cell Biology (S.D.M.),
University of California at Berkeley,
Berkeley, CA 94720

Jonathan J. Urena, BS
Department of Medicine (J.J.U.),
Columbia University College of Physicians and Surgeons,
New York, NY 10032

Whitney Cole, BS
Alesha B. Castillo, PhD
Center for Tissue Regeneration, Repair,
and Restoration (W.C., A.B.C.),
Rehabilitation Research and Development,
Veterans Affairs Palo Alto Health Care System,
Palo Alto, CA 94304

## References

1. Tanaka Y, Inoue T. Fatty marrow in the vertebrae. A parameter for hematopoietic activity in the aged. J Gerontol. 1976 Sep;31(5):527-32.

2. Nishikawa K, Nakashima T, Takeda S, Isogai M, Hamada M, Kimura A, Kodama T, Yamaguchi A, Owen MJ, Takahashi S, Takayanagi H. Maf promotes osteoblast differentiation in mice by mediating the age-related switch in mesenchymal cell differentiation. J Clin Invest. 2010 Oct;120(10):3455-65.

3. Zhou S, Greenberger JS, Epperly MW, Goff JP, Adler C, Leboff MS, Glowacki J. Age-related intrinsic changes in human bone-marrow-derived mesenchymal stem cells and their differentiation to osteoblasts. Aging Cell. 2008 Jun;7(3):335-43.

4. Asumda FZ, Chase PB. Age-related changes in rat bone-marrow mesenchymal stem cell plasticity. BMC Cell Biol. 2011; 12:44.

5. Verma S, Rajaratnam JH, Denton J, Hoyland JA, Byers RJ. Adipocytic proportion of bone marrow is inversely related to bone formation in osteoporosis. J Clin Pathol. 2002 Sep;55(9):693-8.

6. Lu C, Miclau T, Hu D, Hansen E, Tsui K, Puttlitz C, Marcucio RS. Cellular basis for age-related changes in fracture repair. J Orthop Res. 2005 Nov;23(6): 1300-7.

**7.** Ho AD, Wagner W, Mahlknecht U. Stem cells and ageing. The potential of stem cells to overcome age-related deteriorations of the body in regenerative medicine. EMBO Rep. 2005 Jul;6(Spec No):S35-8.

**8.** Nishida S, Endo N, Yamagiwa H, Tanizawa T, Takahashi HE. Number of osteoprogenitor cells in human bone marrow markedly decreases after skeletal maturation. J Bone Miner Metab. 1999;17(3):171-7.

**9.** Burge R, Dawson-Hughes B, Solomon DH, Wong JB, King A, Tosteson A. Incidence and economic burden of osteoporosis-related fractures in the United States, 2005-2025. J Bone Miner Res. 2007 Mar;22(3):465-75.

**10.** U.S. Department of Health and Human Services. Bone Health and Osteoporosis: A Report of the Surgeon General. Rockville, Maryland: U.S. Department of Health and Human Services, Office of the Surgeon General, 2004. Accessed on 2012 Dec 1.http://www.surgeongeneral.gov/library/reports/bonehealth/exec_summ.pdf.

**11.** Eve FS. Abstract of paper on senile changes in bones and some senile diseases of the osseous system. BMJ. 1891;Dec 5(2):1194-5.

**12.** Moerman EJ, Teng K, Lipschitz DA, Lecka-Czernik B. Aging activates adipogenic and suppresses osteogenic programs in mesenchymal marrow stroma/stem cells: the role of PPAR-gamma2 transcription factor and TGF-beta/BMP signaling pathways. Aging Cell. 2004 Dec;3(6):379-89.

**13.** Meunier P, Aaron J, Edouard C, Vignon G. Osteoporosis and the replacement of cell populations of the marrow by adipose tissue. A quantitative study of 84 iliac bone biopsies. Clin Orthop Relat Res. 1971 Oct;80:147-54.

**14.** Zhu M, Kohan E, Bradley J, Hedrick M, Benhaim P, Zuk P. The effect of age on osteogenic, adipogenic and proliferative potential of female adipose-derived stem cells. J Tissue Eng Regen Med. 2009 Jun;3(4):290-301.

**15.** Long MW, Williams JL, Mann KG. Expression of human bone-related proteins in the hematopoietic microenvironment. J Clin Invest. 1990 Nov;86(5):1387-95.

**16.** Bauer TW, Muschler GF. Bone graft materials. An overview of the basic science. Clin Orthop Relat Res. 2000 Feb;(371):10-27.

**17.** de Barros AP, Takiya CM, Garzoni LR, Leal-Ferreira ML, Dutra HS, Chiarini LB, Meirelles MN, Borojevic R, Rossi MI. Osteoblasts and bone marrow mesenchymal stromal cells control hematopoietic stem cell migration and proliferation in 3D in vitro model. PLoS One. 2010;5(2):e9093.

**18.** Chan CK, Chen CC, Luppen CA, Kim JB, DeBoer AT, Wei K, Helms JA, Kuo CJ, Kraft DL, Weissman IL. Endochondral ossification is required for haematopoietic stem-cell niche formation. Nature. 2009 Jan 22;457(7228):490-4.

**19.** Yin T, Li L. The stem cell niches in bone. J Clin Invest. 2006 May;116(5):1195-201.

**20.** Moore KA, Lemischka IR. Stem cells and their niches. Science. 2006 Mar 31;311(5769):1880-5.

**21.** Taichman RS. Blood and bone: two tissues whose fates are intertwined to create the hematopoietic stem-cell niche. Blood. 2005 Apr 1;105(7):2631-9.

**22.** Pittenger MF, Mackay AM, Beck SC, Jaiswal RK, Douglas R, Mosca JD, Moorman MA, Simonetti DW, Craig S, Marshak DR. Multilineage potential of adult human mesenchymal stem cells. Science. 1999 Apr 2;284(5411):143-7.

**23.** Longo KA, Wright WS, Kang S, Gerin I, Chiang SH, Lucas PC, Opp MR, MacDougald OA. Wnt10b inhibits development of white and brown adipose tissues. J Biol Chem. 2004 Aug 20;279(34):35503-9.

**24.** Tamai K, Semenov M, Kato Y, Spokony R, Liu C, Katsuyama Y, Hess F, Saint-Jeannet JP, He X. LDL-receptor-related proteins in Wnt signal transduction. Nature. 2000 Sep 28;407(6803):530-5.

**25.** Gong Y, Slee RB, Fukai N, Rawadi G, Roman-Roman S, Reginato AM, Wang H, Cundy T, Glorieux FH, Lev D, Zacharin M, Oexle K, Marcelino J, Suwairi W, Heeger S, Sabatakos G, Apte S, Adkins WN, Allgrove J, Arslan-Kirchner M, Batch JA, Beighton P, Black GC, Boles RG, Boon LM, Borrone C, Brunner HG, Carle GF, Dallapiccola B, De Paepe A, Floege B, Halfhide ML, Hall B, Hennekam RC, Hirose T, Jans A, Jüppner H, Kim CA, Keppler-Noreuil K, Kohlschuetter A, LaCombe D, Lambert M, Lemyre E, Letteboer T, Peltonen L, Ramesar RS, Romanengo M, Somer H, Steichen-Gersdorf E, Steinmann B, Sullivan B, Superti-Furga A, Swoboda W, van den Boogaard MJ, Van Hul W, Vikkula M, Votruba M, Zabel B, Garcia T, Baron R, Olsen BR, Warman ML; Osteoporosis-Pseudoglioma Syndrome Collaborative Group. LDL receptor-related protein 5 (LRP5) affects bone accrual and eye development. Cell. 2001 Nov 16;107(4):513-23.

**26.** Boyden LM, Mao J, Belsky J, Mitzner L, Farhi A, Mitnick MA, Wu D, Insogna K, Lifton RP. High bone density due to a mutation in LDL-receptor-related protein 5. N Engl J Med. 2002 May 16;346(20):1513-21.

**27.** Qiu W, Andersen TE, Bollerslev J, Mandrup S, Abdallah BM, Kassem M. Patients with high bone mass phenotype exhibit enhanced osteoblast differentiation and inhibition of adipogenesis of human mesenchymal stem cells. J Bone Miner Res. 2007 Nov;22(11):1720-31.

**28.** Mao B, Wu W, Li Y, Hoppe D, Stannek P, Glinka A, Niehrs C. LDL-receptor-related protein 6 is a receptor for Dickkopf proteins. Nature. 2001 May 17;411(6835):321-5.

**29.** Tian E, Zhan F, Walker R, Rasmussen E, Ma Y, Barlogie B, Shaughnessy JD Jr. The role of the Wnt-signaling antagonist DKK1 in the development of osteolytic lesions in multiple myeloma. N Engl J Med. 2003 Dec 25;349(26):2483-94.

**30.** Berenson JR. Biology and management of multiple myeloma. Totowa: Humana Press; 2004. p 369.

**31.** Minear S, Leucht P, Jiang J, Liu B, Zeng A, Fuerer C, Nusse R, Helms JA. Wnt proteins promote bone regeneration. Sci Transl Med. 2010 Apr 28;2(29): 29ra30.

**32.** Laudes M. Role of WNT signalling in the determination of human mesenchymal stem cells into preadipocytes. J Mol Endocrinol. 2011 Apr;46(2):R65-72.

**33.** Duran-Struuck R, Dysko RC. Principles of bone marrow transplantation (BMT): providing optimal veterinary and husbandry care to irradiated mice in BMT studies. J Am Assoc Lab Anim Sci. 2009 Jan;48(1):11-22.

**34.** Greenwald AS. Current concepts in joint replacement. Orthopedics. 2010 Sep; 33(9):626.

**35.** Lustig B, Jerchow B, Sachs M, Weiler S, Pietsch T, Karsten U, van de Wetering M, Clevers H, Schlag PM, Birchmeier W, Behrens J. Negative feedback loop of Wnt signaling through upregulation of conductin/axin2 in colorectal and liver tumors. Mol Cell Biol. 2002 Feb;22(4):1184-93.

**36.** Okabe M, Ikawa M, Kominami K, Nakanishi T, Nishimune Y. 'Green mice' as a source of ubiquitous green cells. FEBS Lett. 1997 May 5;407(3):313-9.

**37.** Minear S, Leucht P, Miller S, Helms JA. rBMP represses Wnt signaling and influences skeletal progenitor cell fate specification during bone repair. J Bone Miner Res. 2010 Jun;25(6):1196-207.

**38.** Bouxsein ML, Radloff SE. Quantitative ultrasound of the calcaneus reflects the mechanical properties of calcaneal trabecular bone. J Bone Miner Res. 1997 May;12(5):839-46.

**39.** Ikawa T, Hirose S, Masuda K, Kakugawa K, Satoh R, Shibano-Satoh A, Kominami R, Katsura Y, Kawamoto H. An essential developmental checkpoint for production of the T cell lineage. Science. 2010 Jul 2;329(5987):93-6.

**40.** Cooper GM, Mooney MP, Gosain AK, Campbell PG, Losee JE, Huard J. Testing the critical size in calvarial bone defects: revisiting the concept of a critical-size defect. Plast Reconstr Surg. 2010 Jun;125(6):1685-92.

**41.** Schmitz JP, Hollinger JO. The critical size defect as an experimental model for craniomandibulofacial nonunions. Clin Orthop Relat Res. 1986 Apr;(205):299-308.

**42.** Syed FA, Ng AC. The pathophysiology of the aging skeleton. Curr Osteoporos Rep. 2010 Dec;8(4):235-40.

**43.** Willert K, Brown JD, Danenberg E, Duncan AW, Weissman IL, Reya T, Yates JR 3rd, Nusse R. Wnt proteins are lipid-modified and can act as stem cell growth factors. Nature. 2003 May 22;423(6938):448-52.

**44.** Staal FJ, Luis TC, Tiemessen MM. WNT signalling in the immune system: WNT is spreading its wings. Nat Rev Immunol. 2008 Aug;8(8):581-93.

**45.** Leucht P, Minear S, Ten Berge D, Nusse R, Helms JA. Translating insights from development into regenerative medicine: the function of Wnts in bone biology. Semin Cell Dev Biol. 2008 Oct;19(5):434-43.

**46.** Takada R, Satomi Y, Kurata T, Ueno N, Norioka S, Kondoh H, Takao T, Takada S. Monounsaturated fatty acid modification of Wnt protein: its role in Wnt secretion. Dev Cell. 2006 Dec;11(6):791-801.

**47.** Zhao L, Rooker SM, Morrell N, Leucht P, Simanovskii D, Helms JA. Controlling the in vivo activity of Wnt liposomes. Methods Enzymol. 2009;465:331-47.

**48.** Morrell NT, Leucht P, Zhao L, Kim JB, ten Berge D, Ponnusamy K, Carre AL, Dudek H, Zachlederova M, McElhaney M, Brunton S, Gunzner J, Callow M, Polakis P, Costa M, Zhang XM, Helms JA, Nusse R. Liposomal packaging generates Wnt protein with in vivo biological activity. PLoS One. 2008;3(8):e2930.

**49.** Dhamdhere GR, Fang MY, Jiang J, Olveda RC, Cheng D, Liu B, Lee K, Mulligan KA, Carlson JC, Ransom RC, Weis WI, Helms JA. Drugging a stem cell compartment using Wnt3a protein as a therapeutic. Unpublished manuscript,, 2012.

**50.** Asciutti S, Akiri G, Grumolato L, Vijayakumar S, Aaronson SA. Diverse mechanisms of Wnt activation and effects of pathway inhibition on proliferation of human gastric carcinoma cells. Oncogene. 2011(Feb 24);30(8):956-66.

**51.** Soleimani M, Nadri S. A protocol for isolation and culture of mesenchymal stem cells from mouse bone marrow. Nat Protoc. 2009;4(1):102-6.

**52.** Kiefer F, Wagner EF, Keller G. Fractionation of mouse bone marrow by adherence separates primitive hematopoietic stem cells from in vitro colony-forming cells and spleen colony-forming cells. Blood. 1991 Nov 15;78(10):2577-82.

**53.** Lee SY, Miwa M, Sakai Y, Kuroda R, Oe K, Niikura T, Matsumoto T, Fujioka H, Doita M, Kurosaka M. Isolation and characterization of connective tissue progenitor cells derived from human fracture-induced hemarthrosis in vitro. J Orthop Res. 2008 Feb;26(2):190-9.

**54.** Muschler GF, Nakamoto C, Griffith LG. Engineering principles of clinical cell-based tissue engineering. J Bone Joint Surg Am. 2004 Jul;86(7):1541-58.

**55.** Neri M, Ricca A, di Girolamo I, Alcala'-Franco B, Cavazzin C, Orlacchio A, Martino S, Naldini L, Gritti A. Neural stem cell gene therapy ameliorates pathology and function in a mouse model of globoid cell leukodystrophy. Stem Cells. 2011 Oct;29(10):1559-71.

**56.** Dominici M, Le Blanc K, Mueller I, Slaper-Cortenbach I, Marini F, Krause D, Deans R, Keating A, Dj Prockop, Horwitz E. Minimal criteria for defining multipotent mesenchymal stromal cells. The International Society for Cellular Therapy position statement. Cytotherapy. 2006;8(4):315-7.

**57.** Jho EH, Zhang T, Domon C, Joo CK, Freund JN, Costantini F. Wnt/beta-catenin/Tcf signaling induces the transcription of Axin2, a negative regulator of the signaling pathway. Mol Cell Biol. 2002 Feb;22(4):1172-83.

**58.** Suire C, Brouard N, Hirschi K, Simmons PJ. Isolation of the stromal-vascular fraction of mouse bone marrow markedly enhances the yield of clonogenic stromal progenitors. Blood. 2012 Mar 15;119(11):e86-95.

**59.** Reinwald S, Burr D. Review of nonprimate, large animal models for osteoporosis research. J Bone Miner Res. 2008 Sep;23(9):1353-68.

**60.** Justesen J, Stenderup K, Ebbesen EN, Mosekilde L, Steiniche T, Kassem M. Adipocyte tissue volume in bone marrow is increased with aging and in patients with osteoporosis. Biogerontology. 2001;2(3):165-71.

**61.** Bigelow CL, Tavassoli M. Fatty involution of bone marrow in rabbits. Acta Anat (Basel). 1984;118(1):60-4.

**62.** Yamamoto M, Takahashi Y, Tabata Y. Enhanced bone regeneration at a segmental bone defect by controlled release of bone morphogenetic protein-2 from a biodegradable hydrogel. Tissue Eng. 2006 May;12(5):1305-11.

**63.** Thornberry NA, Lazebnik Y. Caspases: enemies within. Science. 1998 Aug 28;281(5381):1312-6.

**64.** Cohen GM. Caspases: the executioners of apoptosis. Biochem J. 1997 Aug 15;326(Pt 1):1-16.

**65.** Jiang Y, Jahagirdar BN, Reinhardt RL, Schwartz RE, Keene CD, Ortiz-Gonzalez XR, Reyes M, Lenvik T, Lund T, Blackstad M, Du J, Aldrich S, Lisberg A, Low WC, Largaespada DA, Verfaillie CM. Pluripotency of mesenchymal stem cells derived from adult marrow. Nature. 2002 Jul 4;418(6893):41-9.

**66.** Trowbridge JJ, Guezguez B, Moon RT, Bhatia M. Wnt3a activates dormant c-Kit(-) bone marrow-derived cells with short-term multilineage hematopoietic reconstitution capacity. Stem Cells. 2010 Aug;28(8):1379-89.

**67.** Congdon KL, Voermans C, Ferguson EC, DiMascio LN, Uqoezwa M, Zhao C, Reya T. Activation of Wnt signaling in hematopoietic regeneration. Stem Cells. 2008 May;26(5):1202-10.

**68.** Gregory CA, Gunn WG, Reyes E, Smolarz AJ, Munoz J, Spees JL, Prockop DJ. How Wnt signaling affects bone repair by mesenchymal stem cells from the bone marrow. Ann N Y Acad Sci. 2005 May ;1049:97-106.

**69.** Suda T, Arai F. Wnt signaling in the niche. Cell. 2008 Mar 7;132(5):729-30.

**70.** Prockop DJ, Gregory CA, Spees JL. One strategy for cell and gene therapy: harnessing the power of adult stem cells to repair tissues. Proc Natl Acad Sci U S A. 2003 Sep 30;100(Suppl 1):11917-23.

**71.** Li HX, Luo X, Liu RX, Yang YJ, Yang GS. Roles of Wnt/beta-catenin signaling in adipogenic differentiation potential of adipose-derived mesenchymal stem cells. Mol Cell Endocrinol. 2008 Sep 10;291(1-2):116-24.

**72.** Ross SE, Hemati N, Longo KA, Bennett CN, Lucas PC, Erickson RL, MacDougald OA. Inhibition of adipogenesis by Wnt signaling. Science. 2000 Aug 11;289(5481):950-3.

**73.** Christodoulides C, Laudes M, Cawthorn WP, Schinner S, Soos M, O'Rahilly S, Sethi JK, Vidal-Puig A. The Wnt antagonist Dickkopf-1 and its receptors are coordinately regulated during early human adipogenesis. J Cell Sci. 2006 Jun 15;119(Pt 12):2613-20.

**74.** Takada I, Kouzmenko AP, Kato S. Wnt and PPARgamma signaling in osteoblastogenesis and adipogenesis. Nat Rev Rheumatol. 2009 Aug;5(8):442-7.

**75.** Cawthorn WP, Bree AJ, Yao Y, Du B, Hemati N, Martinez-Santibañez G, MacDougald OA. Wnt6, Wnt10a and Wnt10b inhibit adipogenesis and stimulate osteoblastogenesis through a β-catenin-dependent mechanism. Bone. 2012 Feb;50(2):477-89.

**76.** Rosen CJ, Ackert-Bicknell C, Rodriguez JP, Pino AM. Marrow fat and the bone microenvironment: developmental, functional, and pathological implications. Crit Rev Eukaryot Gene Expr. 2009;19(2):109-24.

**77.** Trudel G, Payne M, Mädler B, Ramachandran N, Lecompte M, Wade C, Biolo G, Blanc S, Hughson R, Bear L, Uhthoff HK. Bone marrow fat accumulation after 60 days of bed rest persisted 1 year after activities were resumed along with hemopoietic stimulation: the Women International Space Simulation for Exploration study. J Appl Physiol. 2009 Aug;107(2):540-8.

**78.** Kirkland JL, Tchkonia T, Pirtskhalava T, Han J, Karagiannides I. Adipogenesis and aging: does aging make fat go MAD? Exp Gerontol. 2002 Jun;37(6):757-67.

**79.** Hall MP, Band PA, Meislin RJ, Jazrawi LM, Cardone DA. Platelet-rich plasma: current concepts and application in sports medicine. J Am Acad Orthop Surg. 2009 Oct;17(10):602-8.

**80.** Oreffo RO. Growth factors for skeletal reconstruction and fracture repair. Curr Opin Investig Drugs. 2004 Apr;5(4):419-23.

**81.** Glassman SD, Gum JL, Crawford CH 3rd, Shields CB, Carreon LY. Complications with recombinant human bone morphogenetic protein-2 in posterolateral spine fusion associated with a dural tear. Spine J. 2011 Jun;11(6):522-6.

**82.** Carragee EJ, Hurwitz EL, Weiner BK. A critical review of recombinant human bone morphogenetic protein-2 trials in spinal surgery: emerging safety concerns and lessons learned. Spine J. 2011 Jun;11(6):471-91.

**83.** Carragee EJ, Mitsunaga KA, Hurwitz EL, Scuderi GJ. Retrograde ejaculation after anterior lumbar interbody fusion using rhBMP-2: a cohort controlled study. Spine J. 2011 Jun;11(6):511-6.

**84.** Whitfield ML, George LK, Grant GD, Perou CM. Common markers of proliferation. Nat Rev Cancer. 2006 Feb;6(2):99-106.

**85.** Rhodes DR, Yu J, Shanker K, Deshpande N, Varambally R, Ghosh D, Barrette T, Pandey A, Chinnaiyan AM. Large-scale meta-analysis of cancer microarray data identifies common transcriptional profiles of neoplastic transformation and progression. Proc Natl Acad Sci U S A. 2004 Jun 22;101(25):9309-14.